

Some Aspects of the Three-Dimensional Interface Cracks Analysis

Jelena M. DJOKOVIĆ, Ružica R. NIKOLIĆ, Jan BUJNAK, Branislav HADŽIMA, Radoljub TOMIĆ

Abstract: Many problems of interfacial cracks are three dimensional in nature. Three-dimensional cracks at an interface of the two materials are analysed in this paper. For a crack at an interface, the stress intensity factors, load phase angle and energy release rate depend on elastic characteristics of two bonded materials and on geometry and the load conditions of a bimaterial sample. Influence of Dundurs' parameters on stress intensity factors, load phase angle and energy release rate for different bi-material combinations and for the quarter-circular corner crack are discussed in this paper. Results show that elastic properties of materials constituting the interface have significant influence on behaviour of the 3D interface crack. Mode I stress intensity factor K_I increases when the crack front approaches the free surface, while K_{II} remains almost constant having the highest values between 10° and 80° , what results in high values of the load phase angle. The K_{III} stress intensity factor is zero in the symmetry plane, while its value increases as the crack front approaches free surfaces. The energy release rate diagrams show that the crack of a quarter circular front propagates faster closer to free surfaces than in the middle what means that the crack front would have the tendency of straightening.

Keywords: Dundurs' parameters; interface cracks; Load Phase angle; Stress intensity factors; Three-dimensional cracks

1 INTRODUCTION

The first papers on the subject of interface cracks were published by Williams [1], who studied the local stress field in the vicinity of semi-infinite interface crack whose faces were force-free. The interface crack lies between the two ideally joined elastic half-spaces. Williams noticed that, unlike for the homogeneous materials, stresses around the interface crack exhibit the oscillatory character. Rice and Shih [2] obtained expressions for the stress field around the interface crack tip and in accordance with those, the elastic stress fields distant from the tip for various problems. Works by Erdogan [3] and England [4] provided new contributions to further investigation of the two-dimensional singular model for one or several cracks in bimaterial systems. In recent times, the progress in investigating the interface static fracture was realized by fundamental work of Rice [5] and others, Hutchinson and Suo [6] and Nikolic and Djokovic [7]. Qu and Bassani [8] analysed the crack at the interface of the two anisotropic materials to define the stress intensity factors (SIFs) according to the stress fields at the crack tip. Nakamura and Kamath [9] analysed 3D crack growth and destruction of a thin film on a rigid substrate. Gosz et al. [10] introduced a new method for determination of mixed mode SIFs along the curved 3D bi-material interface crack. Ayhan et al. [11] developed an efficient computer model, using the enriched finite element at the crack tip, which provides correct results for the asymptotic behaviour at the crack tip. Nagai et al. [13] have determined the stress intensity factors for the 3D interface crack in various anisotropic materials. Koguchi and Yokoyama [14] investigated the singular stress field at interface vertex for 3D joints. Saputra et al. [15] calculated 3D parameters of fracture for the interfacial crack and notches using the scaled boundary finite element method.

Many problems of the interface crack are actually three-dimensional. The interface crack can have three forms: quarter circular, triangular and concave (Fig. 1).

Steel, as a traditional construction material, is in exploitation subjected to wear, corrosion and oxidation. One of the most effective ways of improving its properties is the application of ceramic coatings. The ceramic coatings are often used to protect the base alloys from hot corrosion and

oxidation, as well as to reduce the wear damage. The second function is to reduce the temperature of the base metal in thermal insulation coatings. Among various ceramic materials used to improve steel properties, Al_2O_3 is one of the most widely used, due to its high corrosion resistance, good wear resistance and low price. Coatings made of Al_2O_3 have been widely used in cutting tools, engines, turbines, space vehicles and biomedicine.

The problem of the 3D interface crack between steel and Al_2O_3 coating, for the 3D joint, shown in Fig. 2 was considered in this work.

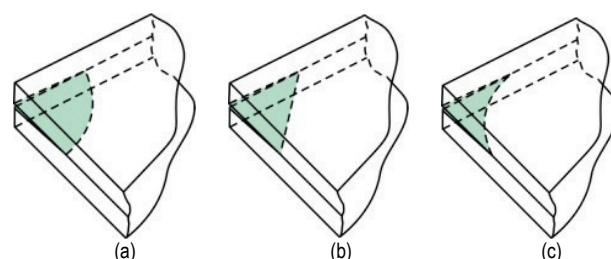


Figure 1 The three possible forms of the 3D interface crack: (a) quarter circular, (b) triangular, (c) concave

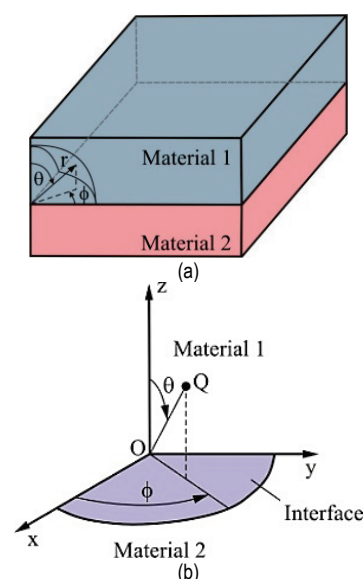


Figure 2 The three-dimensional joint with the crack at the interface (a) and the spherical coordinate system (b)

2 PROBLEM FORMULATION

The stress field singularity appears due to differences in material characteristics at corners of the interface between the two different materials. If an external force acts on such a joint or the environment temperature changes, the crack would appear in the vicinity or at the interface due to this stress singularity. The stress and deformation fields at the interface crack tip have the form:

$$\begin{aligned} (\sigma_{22} + i\sigma_{12})_{\theta=0} &= \frac{(K_I + iK_{II})r^{i\varepsilon}}{\sqrt{2\pi r}}, \quad (\sigma_{23})_{\theta=0} = \frac{K_{III}}{\sqrt{2\pi r}}, \\ \delta_2 + i\delta_1 &= \frac{1}{(1 + 2i\varepsilon)\cosh(\pi\varepsilon)} \cdot \frac{4Kr^{i\varepsilon}}{E_*} \cdot \sqrt{\frac{2r}{\pi}}, \\ \delta_3 &= \frac{2K_{III}}{\mu_*} \cdot \sqrt{\frac{2r}{\pi}}, \\ \varepsilon &= \frac{1}{2\pi} \ln \left(\frac{1-\beta}{1+\beta} \right), \quad \frac{2}{E_*} = \frac{1}{\bar{E}_1} + \frac{1}{\bar{E}_2}, \quad \frac{2}{\mu_*} = \frac{1}{\mu_1} + \frac{1}{\mu_2}, \end{aligned} \quad (1)$$

respectively, where: r is the distance from the crack tip, ε is the mode mixity, β is one of the two Dundurs parameters, Dundurs [16], μ_i is the shear modulus, ν_i is the Poisson's ratio, E_i is Young's elasticity modulus, $\bar{E}_i = E_i / (1 - \nu_i^2)$ is valid for the plane strain state and $\bar{E}_i = E_i$ for the plane stress state, while subscripts $i = 1, 2$ refer to materials above and below the interface.

As can be seen from Eq. (1), the stress field in the vicinity of the interface crack tip is a linear combination of coupled oscillatory field, defined by the complex SIF, $K = K_I + iK_{II}$, and non-oscillatory field, measured by the real SIF, K_{III} . Unlike the case of a homogeneous material, where there exist two separate SIFs for Mode I and Mode II crack propagation conditions, K_I and K_{II} , respectively, for this case, there is one complex SIF for the planar modes; for an interface crack, planar modes are mutually coupled. The interface SIFs are defined in such a way that when materials across the interface are identical $K_I \rightarrow K_I$ and $K_{II} \rightarrow K_{II}$. When $\beta = 0$ and $\varepsilon = 0$, K_I represents the measure of the normal component of the stress singularity, while K_{II} measures the shear component, with usual definition of the stress intensity factors.

Solution for the problem of interface crack is complete either if SIFs K_I , K_{II} and K_{III} are known, or if the energy release rate G and the phase angles ψ and φ are known. The energy release rate for an interface crack is:

$$G = \frac{1}{\cosh^2(\pi\varepsilon)} \cdot \frac{|K|^2}{E_*} + \frac{K_{III}^2}{2\mu_*}. \quad (2)$$

Since $\varepsilon \neq 0$ for the interface crack, influences of tension and shear in the vicinity of crack tip are not separated. To estimate the relative dependence of shear on normal forces, characteristic length L should be known. Now, one can write for the oscillatory field:

$$\tan \psi = \frac{\text{Im}(KL^{i\varepsilon})}{\text{Re}(KL^{i\varepsilon})}, \quad \cos \varphi = \frac{K_{III}}{\sqrt{|K|^2 + K_{III}^2}}. \quad (3)$$

where ψ and φ denote the mixed mode in the K space. The length L is arbitrarily chosen, but for one bimaterial combination it can be invariant, i.e. L may not be dependent on the size and type of the sample. A reasonable choice for value of L is size of the elastic area, depending on the size of a sample. For instance, $L = 100 \mu\text{m}$ is the usual value for majority of brittle bimaterial samples for laboratory research, Shih [17].

3 RESULTS AND DISCUSSION

The normalized SIFs values variations along the crack front are shown in Fig. 3, for the case of a 3D crack of the quarter circular form at the interface $\text{Al}_2\text{O}_3/\text{steel}$, with the following material characteristics $E_1 = 375 \text{ GPa}$, $\nu_1 = 0.27$, $E_2 = 216 \text{ GPa}$, $\nu_2 = 0.28$. The SIFs variation along angle θ , measured from the symmetry axis, and normalized by the solution for the Mode I SIF of a penny-shaped crack $K_{IR} = (2/\pi)\sigma_0\sqrt{\pi a}$.

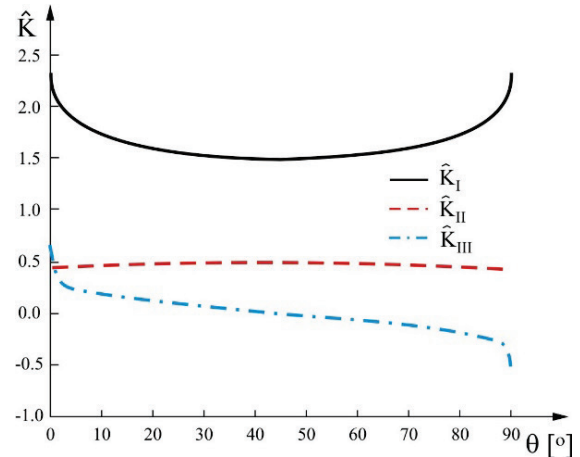


Figure 3 Normalized SIFs variation in terms of angle θ for the 3D crack of the quarter circular form at the $\text{Al}_2\text{O}_3/\text{steel}$ interface.

Fig. 3 indicates that K_I and K_{II} are symmetrical with respect to the $\theta = 45^\circ$ plane, while K_{III} is asymmetrical. Mode I SIF increases as the crack front is closer to the free surface. The Mode II SIF remains almost constant along the whole front. The Mode III SIF is zero in the symmetry plane, and then it increases as the front is getting closer to the free surface, but it also has a negative value.

From Fig. 3 one can notice that all the three SIFs contribute to the energy release rate G , since they are of the same order of magnitude. It can also be seen that the Mode II SIF, although almost constant, has the highest values between 10° and 80° , what has, as a consequence, high values of the load phase angle.

The normalized phase angle variation along the crack front is shown in Fig. 4, for the case of the 3D crack of a quarter circular form at the interface $\text{Al}_2\text{O}_3/\text{steel}$, in terms of angle θ . In Fig. 4 one can notice symmetry of results with respect to the $\theta = 45^\circ$ plane.

Energy release rate (normalized with $G_{IR} = K_{IR}^2 / E_*$) variation along the crack front is shown in Fig. 5, for 3D crack of a quarter circular form at the interface Al_2O_3 /steel. Fig. 5 indicates symmetry of results with respect to the $\theta = 45^\circ$ plane, and the fact that the quarter circular front crack propagates faster near free surfaces than in the centre.

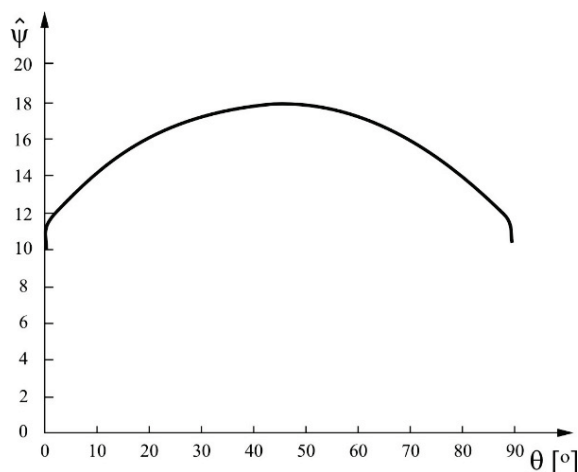


Figure 4 Normalized phase angle variation in terms of angle θ for the 3D crack of a quarter circular form at the Al_2O_3 /steel interface

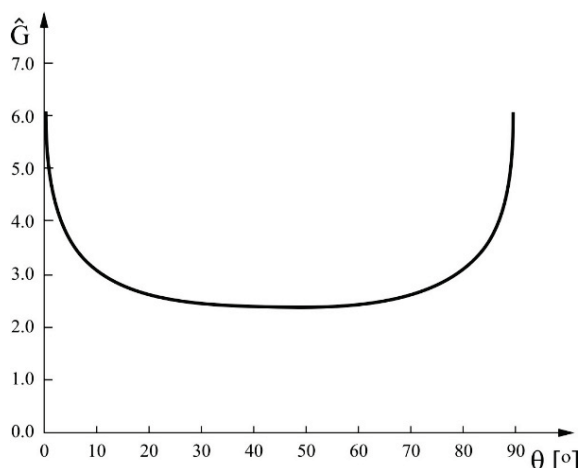


Figure 5 Normalized energy release rate variation in terms of angle θ for the 3D crack of a quarter circular form at the Al_2O_3 /steel interface

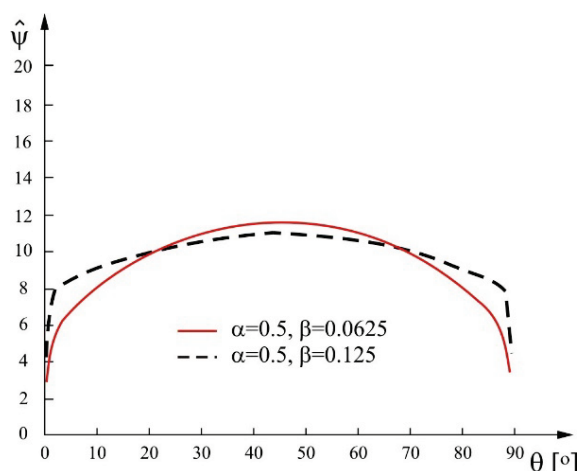


Figure 6 Normalized load phase angle variation in terms of angle θ for 3D crack of a quarter circular form for two arbitrary bimaterial combinations

Considering that for the interface crack, the SIFs, load phase angle and energy release rate depend on the material

characteristics of two materials constituting interface, the normalized load phase angle and energy release rate are shown in Figs. 6 and 7, respectively, for two bimaterial combinations and for the sake of comparison. Two bimaterial combinations, with Dundurs parameters $\alpha = 0.5$ and $\beta = 0.0625$ and $\alpha = 0.5$ and $\beta = 0.125$, were considered.

From variation of the normalized load phase angle in Fig. 6 (about the symmetry plane $\theta = 45^\circ$) one can see that it is significantly affected by material characteristics.

Fig. 7 indicates that the normalized values of the energy release rate increase in the central region with increase in the material elastic characteristics.

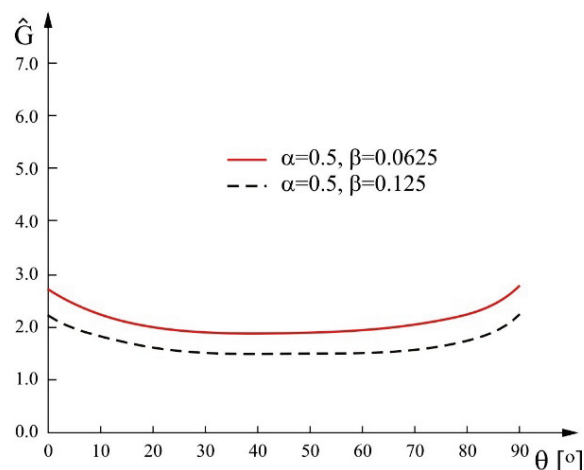


Figure 7 Normalized energy release rate variation along angle θ for 3D crack of a quarter circular form for two arbitrary bimaterial combinations

4 CONCLUSION

Based on presented results, it can be concluded that all three SIFs are contributing to energy release rate G since they are all of the same order of magnitude. In addition, it can be noticed that K_I and K_{II} are symmetrical with respect to the $\theta = 45^\circ$ plane, while K_{III} is asymmetric. The Mode I SIF increases as the crack approaches the free surface. The Mode II SIF remains almost constant along the whole front, but it has the highest values between 10° and 80° , resulting in high values of the load phase angle. The Mode III SIF is zero in the symmetry plane, with increasing value as the front approaches to free surfaces, although its value can be of the negative sign, as well.

Those results also show existence of significant differences in the Mode III SIFs, what has not been taken into account in planar problems.

Based on the energy release rate diagrams, one can see that the crack with the quarter circular front propagates faster closer to free surfaces than in the center. This means that the crack front has the tendency of straightening.

It is also shown that elastic properties of materials constituting the interface have significant influence on behaviour of the 3D interface crack.

Acknowledgements

This research was partially supported by the Ministry of Education, Science and Technological Development of the Republic of Serbia through grants ON174001, ON174004 and TR32036 and by the European regional development fund and Slovak state budget by the project

ITMS2014+313011D011 "Research Centre of the University of Žilina - 2nd phase" and project ITMS2014+313011T426 "Research and development activities of the Žilina University in Žilina for 21st century industry in the field of materials and nanotechnologies"

5 REFERENCES

- [1] Williams, M. L. (1959). The stresses around a fault or crack in dissimilar media. *Bulletin of the Seismological Society of America*, 49, 199-204.
- [2] Rice, J. R. & Sih, G. C. (1965). Plane Problems of Cracks in Dissimilar Media. *ASME Journal of Applied Mechanics*, 32, 418-423. <https://doi.org/10.1115/1.3625816>
- [3] Erdogan, F. (1965). Stress Distribution in Bonded Dissimilar Materials with Cracks. *ASME Journal of Applied Mechanics*, 32, 403-410. <https://doi.org/10.1115/1.3625814>
- [4] England, A. H. (1965). A Crack Between Dissimilar Media. *ASME Journal of Applied Mechanics*, 32, 400-402. <https://doi.org/10.1115/1.3625813>
- [5] Rice, J. R. (1988). Elastic fracture mechanics concepts for interfacial cracks. *ASME Journal of Applied Mechanics*, 55, 98-103. <https://doi.org/10.1115/1.3173668>
- [6] Hutchinson, J. W. & Suo, Z. (1992). Mixed mode cracking in layered materials. *Advances in Applied Mechanics*, 29, 63-191. [https://doi.org/10.1016/S0065-2156\(08\)70164-9](https://doi.org/10.1016/S0065-2156(08)70164-9)
- [7] Nikolic, R. R. & Djokovic, J. M. (2011). Interfacial Cracks in Bicrystals and Bimaterials. In: *Crack Growth: Rates, Prediction and Prevention*, Editor: D. Kubair, Nova Publishers, Inc., New York, 101-126.
- [8] Qu, J. & Bassani, J. L. (1993). Interfacial fracture mechanics for anisotropic biomaterials. *ASME Journal of Applied Mechanics*, 60, 422-431. <https://doi.org/10.1115/1.2900810>
- [9] Nakamura, T. & Kamath, S. M. (1992). Three-dimensional effects in thin film fracture mechanics. *Mechanics of Materials*, 13, 67-77. [https://doi.org/10.1016/0167-6636\(92\)90037-E](https://doi.org/10.1016/0167-6636(92)90037-E)
- [10] Gosz, M., Dolbow, J., & Moran, B. (1998). Domain integral formulation for stress intensity factor computation along curved three-dimensional interface cracks. *International Journal of Solids and Structures*, 35, 1763-1783. [https://doi.org/10.1016/S0020-7683\(97\)00132-7](https://doi.org/10.1016/S0020-7683(97)00132-7)
- [11] Ayhan, A., Kaya, A., & Nied, H. (2006). Analysis of three-dimensional interface cracks using enriched finite elements. *International Journal of Fracture*, 142, 255-276. <https://doi.org/10.1007/s10704-006-9040-7>
- [12] Chaudhuri, R. (2006). Three-dimensional asymptotic stress field in the vicinity of the circumference of a bimaterial penny-shaped interfacial discontinuity. *International Journal of Fracture*, 141, 211-225. <https://doi.org/10.1007/s10704-006-0076-5>
- [13] Nagai, M., Ikeda, T., & Miyazaki, N. (2007). Stress intensity factor analysis of a three-dimensional interface crack between dissimilar anisotropic materials. *Engineering Fracture Mechanics*, 74, 2481-2497. <https://doi.org/10.1016/j.engfracmech.2006.12.027>
- [14] Koguchi, H. & Yokoyama, K. (2015). Stress analysis in three-dimensional joints with a crack at the vertex of the interface, in case of mode II. *Acta Mechanica*, 1-15.
- [15] Saputra, A., Birk, C., & Song, C. (2015). Computation of three-dimensional fracture parameters at interface cracks and notches by the scaled boundary finite element method. *Engineering Fracture Mechanics*, 148, 213-242. <https://doi.org/10.1016/j.engfracmech.2015.09.006>
- [16] Dundurs, J. (1969). Elastic Interaction of Dislocations with Inhomogeneities, In: *Mathematical Theory of Dislocations*, Editor: T. Mura, ASME, New York, 77-114.
- [17] Shih, C. F. (1991). Cracks on bimaterial interfaces: Elasticity and Plasticity aspects. *Material Science and Engineering*, A143, 77-90. [https://doi.org/10.1016/0921-5093\(91\)90727-5](https://doi.org/10.1016/0921-5093(91)90727-5)

Contact information:

Jelena M. DJOKOVIĆ, PhD, Professor
Technical Faculty in Bor, University of Belgrade
V. Jugoslavije 12, 19210 Bor, Serbia
E-mail: jelenamdjokovic@gmail.com

Ružica R. NIKOLIĆ, PhD, Professor
Research Center, University of Žilina
Univerzitná 1, 010 26 Žilina, Slovakia
E-mail: ruzicamikolic@yahoo.com

Jan BUJNAK, PhD, Professor
Faculty of Civil Engineering, University of Žilina
Univerzitná 1, 010 26 Žilina, Slovakia
E-mail: jan.bujnak@fstav.uniza.sk

Branislav HADZIMA, PhD, Professor
Research Center, University of Žilina
Univerzitná 1, 010 26 Žilina, Slovakia
E-mail: branislav.hadzima@rc.uniza.sk

Radoljub TOMIĆ, PhD, Professor
University "Union - Nikola Tesla"
Faculty for Strategic and Operational Management
Staro sajmište 29, 11070 Belgrade, Serbia
E-mail: tomic_radoljub@yahoo.com